Available online at www.sciencedirect.com
ScienceDirect
Journal of Nuclear Materials 363–365 (2007) 581–585
journal of nuclear materials
www.elsevier.com/locate/jnucmat

Transport barrier fluctuations governed by SOL turbulence spreading

Ph. Ghendrih [a,*], Y. Sarazin [a], G. Ciraolo [a], G. Darmet [a], X. Garbet [a], V. Grangirard [a], P. Tamain [a], S. Benkadda [b], P. Beyer [b]

[a] Association Euratom-CEA, DRDF/DSM/CEA, CEA Cadarache, F-13108 St. Paul-lez-Durance cédex, France
[b] UMR 6633 PIIM CNRS-Université de Provence, 13397 Marseille, France

Abstract

Turbulence spreading, namely turbulent transport extending into a stable region is reported both for the flat density profiles in the far SOL and into a modeled H-mode barrier. It is shown that due to turbulence penetration, the pedestal width fluctuates and that its effective width is a factor 2 smaller than the linear predicted width. Turbulence overshooting throughout the pedestal leads to a non-vanishing turbulent transport within the barrier and provides a coupling of core and SOL turbulence despite the transport barrier.

PACS: 05.60.−k; 52.25.Fi; 52.35.Ra; 52.55.Dy

Keywords: Edge transport; Plasma turbulence; Edge pedestal; Turbulence spreading; Ballistic transport

1. Introduction

Plasma turbulence plays a major role in determining the plasma properties that govern plasma–wall interaction in fusion devices [1]. A striking example is given by the SOL width that is governed by cross-field transport. The later thus determines the area where plasma–wall interaction occurs as well as the plasma temperature and density, both being essential in all atomic processes that are crucial in edge plasma physics. SOL turbulence is also of interest for core physics since the latter will not only depend on plasma mean density and temperatures, as would be the case in a usual boundary layer problem, it will also respond to the turbulence level in the SOL. Although not explicitly stated, this issue is usually considered to be solved by the existence on the edge transport barrier, also referred to as the H-mode barrier or pedestal. The latter does not only yield a benefit in terms of stored energy, it also decouples the core and edge plasma turbulence. The aim of this paper is to analyse the impact of the so-called turbulence spreading, and in particular of SOL turbulence spreading, on the properties of the transport barrier.

Turbulent transport in both the plasma core and plasma edge has long been considered as a local

* Corresponding author.
E-mail address: philippe.ghendrih@cea.fr (Ph. Ghendrih).

0022-3115/$ - see front matter © 2007 Elsevier B.V. All rights reserved.
doi:10.1016/j.jnucmat.2006.12.034

response to macroscopic parameters, typically mean gradients or flows. However, turbulence spreading [2–4] will govern the interplay between stable and unstable regions, and, as a consequence, will lead to a non-local dependence of transport properties. Regarding the edge region, turbulence penetration into the H-mode barrier can change the effective width of the barrier and its scaling properties. Another issue is the existence of strong intermittent transport towards the outer SOL in regions where the mean gradients are found to flatten out. In such areas the plasma should be close to thermodynamical equilibrium and therefore stable. This discrepancy can also be resolved in terms of turbulent spreading into the distant SOL.

Spreading of SOL turbulence is analysed with the flux driven code 'Tokam' [5]. This is a 2D non-linear code for the density and electric potential governed by the interchange instability. Although this model is in good agreement with many facets of SOL turbulence as reported from the experiments, we do not claim that it is the ultimate model to explain all transport properties. Rather, it is a powerful tool to determine key concepts that stem from the non-linear properties of turbulence. The paper is organised in two main Sections. In Section 2, the turbulence model is described and its non-linear transport properties are noted. These provide the basis for the analysis of turbulence spreading into the far SOL. The investigation of spreading properties on transport barriers is addressed in Section 3.

2. Turbulence spreading in 2D interchange turbulence in the SOL

SOL turbulence differs with respect to core turbulence as a result of the sheath boundary conditions that strongly reduce the parallel current flowing on each SOL flux tube. Regimes with reduced parallel current are then very sensitive to charge separation via the curvature drift since the parallel current is less effective to balance the charge separation. Sheath resistivity has been proposed to explain the very large fluctuation levels reported in the SOL [6,7]. We consider here this model of SOL turbulence in the limit $T_i \ll T_e$ with constant T_e. In this model two balance equations are used, the particle balance that governs the density transport, and the charge balance which takes the form of an evolution equation for the vorticity $\Delta\phi$ due to the ion inertia terms, where ϕ is the electric potential. Averaging along a field line in the flute limit, hence with weak parallel gradients, is also performed. The system is then reduced to a $2D(r,\theta)$, and two field model, n the density and ϕ the plasma potential normalised to T_e/e. In these equations time is normalised to the ion Larmor frequency and space is normalised to the so-called hybrid Larmor radius ρ_s, hence $x = (r-a)/\rho_s$ in the radial direction and $y = a\theta/\rho_s$ in the poloidal direction, a being the plasma minor radius.

$$\left(\frac{\partial}{\partial t} - D\nabla_\perp^2 + \{\phi\}\right) n = -\sigma_n n + S, \tag{1}$$

$$n\left(\frac{\partial}{\partial t} - \nu\nabla_\perp^2 + \{\phi\}\right)\nabla_\perp^2\phi + g\partial_y n = \sigma_\phi n. \tag{2}$$

The non-linear terms associated with the spatial dependence of the density n in the left hand side of Eq. (2) are not taken into account. D and ν stand for the collisional transverse diffusion and viscosity (normalised to the Bohm values), S is the particle source term, here localised radially and constant in time and y. σ_n and σ_ϕ are the sheath controlled particle flux and current to the wall, $\sigma_n = \sigma\exp(\Lambda - \phi)$ and $\sigma_\phi = \sigma(1 - \exp(\Lambda - \phi))$, where $\sigma = M_\parallel \rho_s/qR$ is the normalised ion saturation current ($M_\parallel$ being the Mach number of the flow at the plasma sheath, $M_\parallel \sim 1$). The parameter Λ stands for the normalised floating potential and only enforces the electric potential to fluctuate in the vicinity of Λ to minimise the plasma current flowing through the sheath. The operator $\{\phi\}F = \partial_x\phi\partial_y F - \partial_y\phi\ \partial_x F$ is the electric drift convection term. To first order in the fluctuation magnitude, sheath loss terms can be linearised to yield the Hasegawa–Wakatani coupling term $\sigma(n-\phi)$ [8].

Large simulations with $512\rho_s$ in both the radial and poloidal directions have been performed for more than 200 SOL confinement times (typically 1500 turbulence correlation times) [9,10]. In [10], the propagation of the turbulent front is investigated with a prescribed initial density profile characterised by a narrow peak and an extended flat profile. In the simulation, the steep density profile is split by the turbulence into fronts [11]. These fronts propagate into a region with flat density profile with a ballistic motion at constant velocity, typically $M_{\text{front}} = 0.04$. Each density front is associated to an electrostatic dipole that propagates at the same velocity. Turbulence is therefore generated by an unstable density gradient and then overshoots into a stable density region. This is reminiscent of the physics reported in experimental observations

in the deep SOL [12] with intermittent turbulent transport in regions with flat density profiles. Thus, turbulence spreading, i.e. the existence of turbulent transport in regions that are linearly stable, does seem to play a role in SOL turbulence.

3. Reduction of transport barrier width governed by SOL turbulence spreading

Turbulence spreading, when considering the interplay between SOL turbulence and the H-mode transport barrier (or pedestal), will also change the properties of the pedestal. A comprehensive analysis is not possible since one lacks of a complete theoretical understanding of the onset of the H-mode transport barrier. Rather than driving a barrier with a sheared flow, such as in [13], we propose here to analyse the spreading effect in a very artificial transport barrier achieved by setting g in Eq. (2) to 0 over a chosen radial extent Δ_{linear} here set at $32\rho_s$. (Another consequence of the chosen model is that the transport barrier is located in the SOL.)

The barrier is then governed by a linear analysis criterion rather than a complex non-linear effect that can be expected to be specifically sensitive to turbulence spreading. The linear analysis presented in Fig. 1 is performed with equal poloidal and radial wave vectors ($2\pi/15$) that maximise the growth rate and a prescribed density gradient, $\nabla n/n|_{\text{linear}} = \langle \nabla n/n \rangle - 5(\text{r.m.s.}\ (\nabla n/n))$ where r.m.s. $(\nabla n/n)$ is the root mean square of the fluctuating density gradient. With the chosen parameters for this simulation, one finds that the turbulence is sub-critical, namely that the mean density gradient is smaller than the critical density gradient $|\nabla n/n|^* = |\langle \nabla n/n \rangle| + 2.55(\text{r.m.s.}\ (\nabla n/n))$ that is required to destabilise the modes that govern the turbulent transport. The turbulent activity that is sustained can therefore be considered as penetration of turbulence into a stable medium, a situation that is comparable to the spreading of turbulence into the flat density SOL discussed in the previous section.

In the simulations, the effective pedestal width is analysed in terms of an indicator, namely the ratio of the radial turbulent flux $\Gamma_{\text{turb}} = -\partial_y \phi n$ to the mean value of the total radial flux $\langle \Gamma_{\text{total}} \rangle_{(y,t)}$, $I(x,y,t) = \Gamma_{\text{turb}}/\langle \Gamma_{\text{total}} \rangle_{(y,t)}$. Where the average is both a poloidal angle (y) and time average and where $\Gamma_{\text{total}} = \Gamma_{\text{turb}} - D\partial_x n$. This indicator allows one to discriminate regions with large turbulent fluxes $|I| \gtrsim 1$ from that with weak turbulent flux. The indicator $I(x,y,t)$ is proportional to Γ_{turb}, and, as such exhibits large fluctuations with a skewed probability distribution function (PDF) [9,10]. The radial profile of the time and poloidal average of this indicator $\langle I(x,y,t) \rangle_{(y,t)}$ shows a clear signature of the transport barrier. Indeed, while $\langle I(x,y,t) \rangle_{(y,t)} \approx 1$ away from the barrier, $\langle I(x,y,t) \rangle_{(y,t)}$ is significantly reduced within the pedestal, Fig. 2. It drops from the order of 98% to less than 3% but departs significantly from the square shape that would result from a linear analysis, Fig. 1. Associated with the decrease of the turbulent flux, one observes a steepened density gradient, see Fig. 1, leading to a standard tanh-like profile.

The evolution of the poloidally averaged indicator $\langle I \rangle_y$ is shown on Fig. 3. In this $2D$ plot, significant fluctuations of the turbulent flux are observed away from the $g = 0$ region, within $x = (80 \pm 16)\rho_s$, and a drop of the turbulent flux inside this region. The contour line associated with $\langle I(x,y,t) \rangle_{(y,t)}$ values of 0.25 exhibits large fluctuation of its radial location with time, both towards the core (bottom) and to the edge (top). The number of occurrences distribution function (NDF) for these two boundaries is plotted on Fig. 4. The NDF of

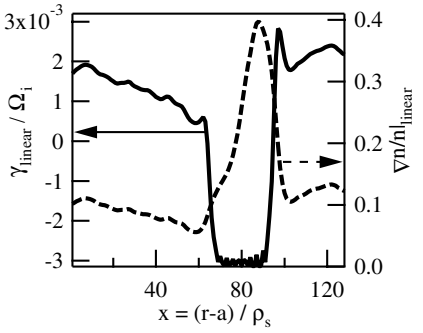

Fig. 1. Radial profile of the linear growth rate γ_{linear}, left axis, computed with the density gradient $\nabla n/n|_{\text{linear}}$, right axis.

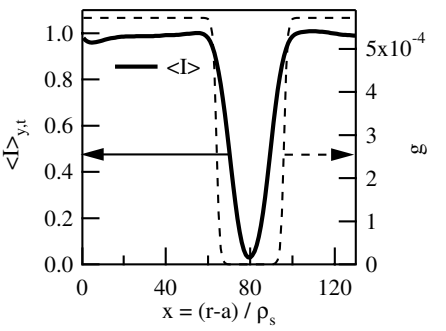

Fig. 2. Radial profile of the mean turbulence indicator $\langle I(x,y,t) \rangle$, left axis, and of the curvature drive g, right axis.

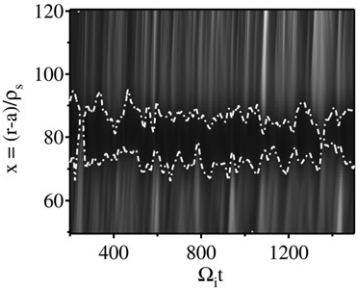

Fig. 3. 2D map of $\langle I\rangle_y$, white for $\langle I\rangle_y \sim 4$, black for 0. The contour $\langle I\rangle_y = 0.25$ is indicated by the dotted lines.

the location of the minimum value of $\langle I\rangle_y$ is also plotted. It exhibits a near gaussian distribution function centred in the middle of the $g = 0$ region. The fluctuation of this position is of the order of $3\rho_s$ slightly smaller than that of the two edges of the transport barrier, typically $4\rho_s$. More interesting are the $10\rho_s$ inward shifts in the mean values of the barrier edges and the skewness of the two NDFs, of the order of 0.3, but with opposite signs, hence both towards the centre of the $g = 0$ region. These two distributions overlap which corresponds in general to events such that both edges of the barrier collapse to the vicinity of centre of the $g = 0$ region. This leads to a transient loss of efficiency of the transport barrier. This analysis indicates that the barrier width is a fluctuating quantity. Its PDF shows that it is reduced from the linear relevant value of $\Delta_{\text{linear}} = 32\rho_s$ to $\Delta_{NL} = 15\rho_s \pm 5\rho_s$. The effect of the skewness of the PDFs of the two edges of the barrier, of order 0.3, leads to a statistical distortion of the barrier width of the order of $2.5\rho_s$. This is at lowest order in agreement with the PDF of the barrier width, but cannot explain the number of occurrences of vanishing barrier widths (typically 1% of the data) as observed on Fig. 3.

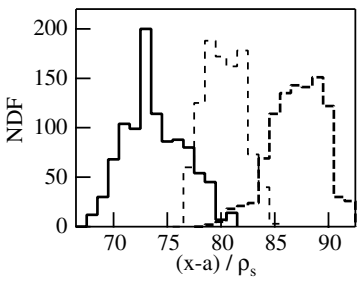

Fig. 4. NDF of the pedestal boundary position, outer (solid line) and inner (dotted line on the right) boundary. The light dashed curve is the NDF of the location of the minimum of $\langle I\rangle_y$.

This statistical analysis leads to a picture of a fluctuating barrier width, the two edges being in first approximation uncorrelated but for very few events, associated with very large fronts burning through the barrier. Therefore, both turbulence penetration, that reduces the barrier width by a factor 2, and turbulence overshoot, that sustains a non-vanishing turbulent transport through the barrier, are at play. A straightforward understanding of this effect can be obtained by considering fronts that propagate radially and that are damped away in the $g = 0$ region with a characteristic time given by the inverse of the linear growth rate $1/\gamma_{\text{linear}}$. The penetration into the $g = 0$ region of a given front with radial velocity v_{Ex} will then be given by $\Lambda_{\text{turb}} = v_{Ex}/\gamma_{\text{linear}}$. The statistical analysis of the radial velocity uphill of the $g = 0$ region allows one to compute Λ_{turb} for each turbulent event, Fig. 5. The r.m.s. value of this penetration depth is $8\rho_s$. This value is in good agreement with the average $10\rho_s$ inward shift of the barrier edge reported above. The slight mismatch can be explained by the fact that the statistics for the barrier location are a poloidal average between the density and radial velocity fluctuations while all velocity fluctuations are considered in Fig. 5. The large values that are reached by Λ_{turb}, up to $20\rho_s$, indicate that only a moderate correlation between uphill and downhill overshooting events will lead to barrier burn through.

The evidence discussed above leads to the picture of turbulent spreading into the transport barrier. When analysing the radial correlation length, one finds that the spreading effect also modifies the turbulent behaviour outside of the $g = 0$ region. The radial variation of this correlation length L_x exhibits three slopes in contrast to the case with no barrier where the radial correlation length is nearly constant. At $40\rho_s$ uphill from the barrier the correlation length exhibits a slow decrease. At a distance comparable to $L_x \sim 15\rho_s$ from the barrier, L_x exhib-

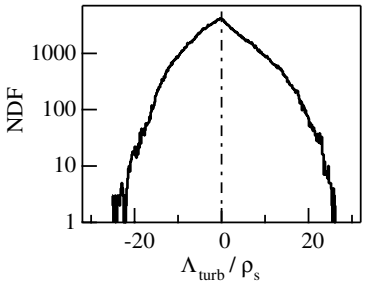

Fig. 5. NDF of the penetration depth of ballistic fronts. The x-axis scale is set at $\pm\Delta_{\text{linear}}$.

its a rapid decrease to $L_x \lesssim 5\ \rho_s$ in the transport barrier where the statistics become too scarce to provide a correct value of L_x. The existence of a transport barrier tends to lower the turbulence over $L_x \sim 15\rho_s$ both uphill and downhill from the transport barrier.

4. Discussion and conclusion

The investigation of turbulence spreading presented in this paper indicates that this effect must play an important role in the SOL transport. In particular, the propagation of turbulent fronts from an area with strong density gradient into a region with flat density profile is characteristic of turbulence spreading. The observation of similar signatures in experiments, namely turbulent transport in the deep SOL with flat density profiles, tends to confirm this analysis. A similar observation is drawn from the analysis of the mean density gradient and the critical density gradient in the simulations. One finds that the critical density gradient is larger than the mean density gradient, so that the average profile is linearly stable, i.e. the turbulence is sub-critical.

Turbulent spreading with respect to a transport barrier is investigated using an artificial transport barrier by setting the curvature drift to 0 ($g = 0$) in a prescribed radial region, with radial extent Δ_{linear}. The two facets of turbulence spreading are then observed. First, turbulence penetration into the transport barrier that reduces the effective width of the transport barrier, by a factor 2, and governs fluctuations of the barrier position and width. Second, turbulent overshoot of the large fronts leads to burn through events where turbulent eddies propagate throughout the transport barrier. The latter effect results in a non-vanishing transport within the transport barrier. Last, when analysing the radial correlation length, one finds that turbulence is modified on both sides of the transport barrier over a radial extent comparable to the unperturbed correlation length, typically $15\rho_s$.

As a consequence, both the barrier width as well as the remnant turbulent transport within the transport barrier will depend on the turbulent activity, both in the plasma core and in the SOL. Such a non-linear spreading effect could be a major difficulty when investigating the scaling laws of the pedestal width and H-mode threshold. These quantities are likely to depend on the SOL turbulence, for which, up to date, the empirical scaling law approach has as yet proven to be unsuccessful. The transport within the barrier itself, and in particular the balance between the electron and ion channels, should also exhibit a dependence on the SOL turbulence. Another consequence of the turbulence overshoot throughout the barrier is the coupling of the core and SOL turbulence despite the H-mode transport barrier. In order to quantify the spreading effect on the pedestal physics, further investigation of the non-linear coupling between the stabilisation and spreading mechanisms will have to be addressed.

Acknowledgements

The authors are most indebted to Professor P. Diamond and Professor D. Hughes for stimulating discussions during the 2005 Festival de Théorie.

References

[1] V. Naulin, these Proceedings, doi:10.1016/j.jnucmat.2006.12.058.
[2] T.S. Hahm et al., Phys. of Plasmas 12 (2005) 090903.
[3] V. Naulin et al., Phys. of Plasmas 12 (2005) 122306.
[4] O.D. Gurcan et al., Phys. of Plasmas 13 (2006) 052306.
[5] S. Benkadda et al., Contr. Plasma Phys. 34 (1994) 247.
[6] A.V. Nedospasov, Sov. J. Plasma Phys. 15 (1989) 659.
[7] X. Garbet et al., Nucl. Fusion 31 (1991) 967.
[8] M. Wakatani et al., Phys. Fluids 27 (1984) 611.
[9] Y. Sarazin, Ph. Ghendrih, Phys. of Plasmas 5 (1998) 4214.
[10] Ph. Ghendrih et al., Nucl. Fusion 43 (2003) 013.
[11] Ph. Ghendrih et al., J. Nucl. Mater. 337339 (2005) 347.
[12] B. LaBombard et al., Phys. Plasmas 8 (2001) 2107.
[13] P. Beyer et al., Phys. Rev. Lett. 94 (2005) 105001.